hep-ph/0006212

June, 2000
OU-HEP-352

Polarized Structure Functions $g_2(x)$ in the Chiral Quark Soliton Model

M. Wakamatsu[1]

Department of Physics, Faculty of Science,
Osaka University,
Toyonaka, Osaka 560-0043, JAPAN

PACS numbers : 12.39.Fe, 12.39.Ki, 12.38.Lg, 13.60.Hb, 14.20.Dh

Abstract

The spin-dependent structure functions $g_2(x, Q^2)$ are investigated within the framework of the chiral quark soliton model. It turns out that the twist-3 part of $g_2(x, Q^2)$ gives nonnegligible contributions to the total distributions at the energy scale of $Q^2 = 5\,\mathrm{GeV}^2$ but mainly in the smaller x region only, so that the corresponding third moments $\int_0^1 x^2\, \bar{g}_2(x, Q^2)\, dx$ are pretty small for both of the proton and neutron in conformity with the recent E155 data.

In our opinion, the unexpectedly small quark spin fraction of the nucleon indicated by the EMC experiment [1] and the light flavor sea-quark asymmetry revealed by the NMC measurement [2] are two remarkable discoveries in the field of nucleon structure function physics. Undoubtedly, both are manifestation of nonperturbative QCD dynamics imbedded in the physics of high-energy deep-inelastic scatterings. An outstanding feature of the chiral quark soliton model (CQSM) is that it can explain both of these observations without recourse to any fine-tuning. (This potentiality of the CQSM was already noticed in [3,4].) In fact, we have already shown that it reproduces all the qualitatively noticeable features of the recent high-energy measurements, including the NMC data for $F_2^p(x) - F_2^n(x)$, $F_2^n(x)/F_2^p(x)$ [2], the Hermes and E866 data for $\bar{d}(x) - \bar{u}(x)$ [8,9], the EMC and SMC data for $g_1^p(x)$, $g_1^n(x)$ and $g_1^d(x)$ [10,11,12,13], in no need of adjustable parameters except for the starting energy scale of the renormalization-group evolution equation [5,6,7].

[1]Email : wakamatu@miho.rcnp.osaka-u.ac.jp

Encouraged by this success, we now push on with our analyses to the twist-3 parton distributions in the nucleon. It is well known that, altogether, there are three twist-3 distribution functions – chiral odd, $e(x,Q^2)$ and $h_L(x,Q^2)$, and chiral-even, $g_2(x,Q^2)$. They are generally believed to provide us with valuable information on quark-gluon correlations in hadrons. In the present investigation, we shall focus our attention on $g_2(x,Q^2)$. There already exist several theoretical investigations of the polarized structure functions $g_2(x,Q^2)$. The most of those are based on various modifications of the MIT bag model as well as its original version [14, 15, 16, 17, 18]. There also exists an investigation based on the Nambu-Jona-Lasinio soliton model [19], which is essentially equivalent to the CQSM. Confining to the lower moments of $g_2(x,Q^2)$, also available are theoretical predictions based on the QCD sum rule [20,21] as well as the quenched lattice QCD [22], etc.

Although based on essentially the same model as [19], the present investigation goes far beyond the previous one in many respects. First, the polarization effects of the negative-energy Dirac-sea quarks in the hedgehog mean-field are fully taken into account. This is very important for offering any reliable predictions for antiquark distributions. Secondly, we also include the novel $1/N_c$ correction (or the first order rotational correction in the collective angular velocity Ω) to the isovector distribution functions. Without inclusion of it, some fundamental isovector observables like the nucleon isovector axial coupling constant would be largely underestimated, thereby being led to the so-called "g_A problem" in the hedgehog soliton model [23, 24]. Thirdly, the nonlocality effects (in time) inherent in the theoretical definition of parton distributions are treated in a consistent way [5, 25].

We start with the following definition of the distribution functions :

$$g_1^{(I=0/I=1)}(x) = \frac{1}{2M}\int_{-\infty}^{\infty}\frac{d\lambda}{2\pi}\,e^{\,i\lambda\,x}\,\langle PS\,|\,\psi^\dagger(0)\,(1+\gamma^0\,\gamma^3)\,\gamma_5\left\{\begin{array}{c}1\\ \tau_3\end{array}\right\}\psi(\lambda\,n)\,|\,PS\rangle\,, \quad (1)$$

$$g_T^{(I=0/I=1)}(x) = \frac{1}{2M}\int_{-\infty}^{\infty}\frac{d\lambda}{2\pi}\,e^{\,i\lambda\,x}\,\langle PS_\perp\,|\,\psi^\dagger(0)\,\gamma^0\,\gamma_\perp\,\gamma_5\left\{\begin{array}{c}1\\ \tau_3\end{array}\right\}\psi(\lambda\,n)\,|\,PS_\perp\rangle\,, \quad (2)$$

which is just standard except for the isospin dependence explained below. Here the parts containing 1 and τ_3 respectively give isoscalar ($I=0$) and isovector ($I=1$) combinations of the relevant distributions. They are normalized such that the corresponding quark distributions $g_T^{(q)}(x)$ with $q=u,d$ are given as

$$g_T^{(u/d)}(x) = \frac{1}{2}\,[\,g_T^{(I=0)}(x) \pm g_T^{(I=1)}(x)\,] \qquad (0<x<1), \quad (3)$$

and similarly for $g_1(x)$. The distribution functions (1) and (2) are formally defined in the region $-1<x<1$. The functions with negative x are to be interpreted as giving antiquark distributions $g_T^{(q)}(x)$ with $q=\bar{u},\bar{d}$ according to the rule :

$$g_T^{(\bar{u}/\bar{d})}(x) = \frac{1}{2}\,[\,g_T^{(I=0)}(-x) \pm g_T^{(I=1)}(-x)\,] \qquad (0<x<1)\,, \quad (4)$$

and similarly for $g_1(x)$. The corresponding structure functions for the proton and the neutron at the model energy scale are then constructed as

$$g_T^{(p/n)}(x) \;=\; \frac{5}{36}\,[\,g_T^{(I=0)}(x) + g_T^{(I=0)}(-x)\,] \;\pm\; \frac{1}{18}\,[\,g_T^{(I=1)}(x) + g_T^{(I=1)}(-x)\,]\,. \tag{5}$$

The twist-2 distribution functions $g_1(x)$ were already evaluated in [5, 6]. The distribution functions $g_T^{(I=0)}(x)$ and $g_T^{(I=1)}(x)$ can be evaluated within the same theoretical framework. Skipping the detail, here we only recall the fact that the isoscalar and isovector parts have totally different dependences on the collective angular velocity Ω of the rotating hedgehog mean field, which itself scales as $1/N_c$ [5] :

$$g_T^{(I=0)}(x) \;\sim\; N_c\,O(\Omega^1) \;\sim\; O(N_c^0)\,, \tag{6}$$

$$g_T^{(I=0)}(x) \;\sim\; N_c\,[\,O(\Omega^0) \;+\; O(\Omega^1)\,] \;\sim\; O(N_c^1) + O(N_c^0)\,. \tag{7}$$

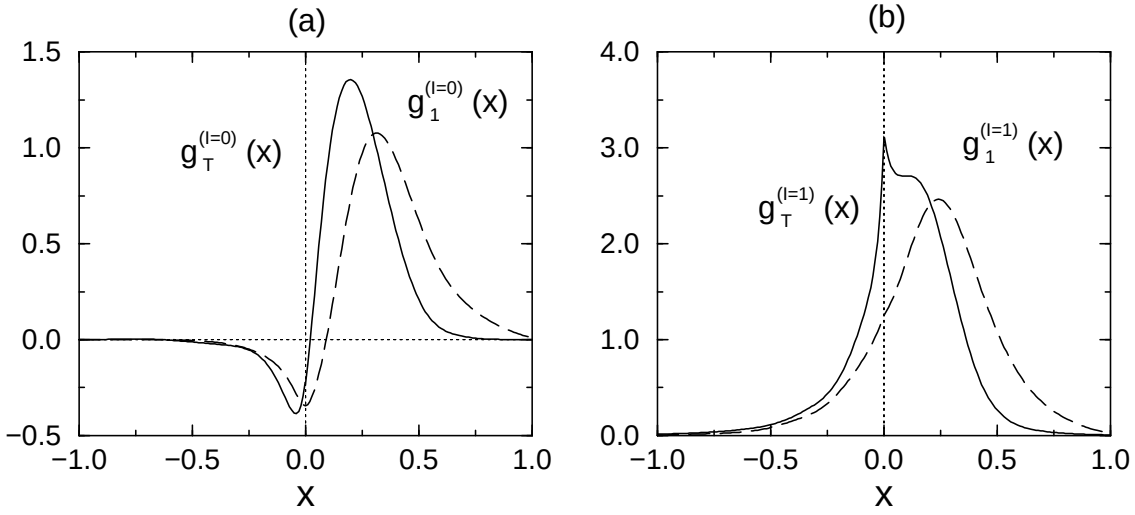

Figure 1: (a) The isoscalar parts of the distribution functions $g_1(x)$ and $g_T(x)$. (b) The isovector parts of $g_1(x)$ and $g_T(x)$.

Shown in Fig.1 are the results for $g_T^{(I=0)}(x)$ and $g_T^{(I=1)}(x)$ in comparison with the twist-2 distributions $g_1^{(I=0)}(x)$ and $g_1^{(I=1)}(x)$. We first point out that the isoscalar and isovector distributions have totally dissimilar shapes reflecting quite different N_c-dependence given in (6) and (7). Next, comparing $g_T^{(I=0)}(x)$ and $g_1^{(I=0)}(x)$, one finds that the $g_T^{(I=0)}(x)$ has a peak at smaller value of x than $g_1^{(I=0)}(x)$ and damps faster as x increases. The same tendency is also observed for the isovector distributions, but in this case the concentration of the distribution $g_T^{(I=1)}(x)$ into the smaller x region is even more profound. This is due to more significant

effect of vacuum polarization, which is peaked around $x \simeq 0$. It means that the "valence-quark-only" approximation adopted in [19] cannot be justified at least for $g_T^{(I=1)}(x)$ and to a lesser extent also for $g_1^{(I=1)}(x)$. Note, however, that the vacuum polarization contributions, which are dominant in the smaller x region, are partially canceled in the corresponding spin structure function $g_2^{(I=1)}(x)$ defined as a difference of $g_T^{(I=1)}(x)$ and $g_1^{(I=1)}(x)$. In any case, we emphasize the following. The CQSM gives fairly different predictions for the shapes of $g_1(x)$ and $g_T(x)$. Moreover, the shapes of both distributions are strongly dependent on the isospin (or more generally flavor) combinations. Furthermore, both distributions $g_1^{(I=1)}(x)$ and $g_T^{(I=1)}(x)$ have large support in the negative x region, which implies sizable flavor asymmetry of the spin-dependent sea-quark (antiquark) distributions [6, 26].

To compare these predictions of the CQSM with the existing high-energy data for $g_2^p(x, Q^2)$ and $g_2^d(x, Q^2)$, we must take account of the scale dependence of the distribution functions. We have done it as follows. Remember first that the spin structure function $g_2(x, Q^2)$ is defined as a difference of $g_T(x, Q^2)$ and $g_1(x, Q^2)$, i.e. $g_2(x, Q^2) = g_T(x, Q^2) - g_1(x, Q^2)$. (In the following discussion on the scale dependence, we omit the isospin indices for the structure functions, for notational simplicity.) The Burkhardt-Cottingham sum rule [27] holds exactly, i.e.

$$\int_0^1 g_2(x, Q^2)\, dx \;=\; 0\,, \tag{8}$$

if the charges (or the first moments) of $g_1(x, Q^2)$ and $g_T(x, Q^2)$ are equal, which in turn follows from the rotational invariance of the whole theoretical scheme. This property is automatically satisfied in usual low energy models like the MIT bag model [14,15,16,17,18] or the CQSM [19]. The $g_2(x, Q^2)$ is further decomposed into the twist-2 (Wandzura-Wilczek) part and the genuine twist-3 part as [28]

$$g_2^{WW}(x, Q^2) \;\equiv\; -\, g_1(x, Q^2) \;+\; \int_x^1 \frac{dy}{y}\, g_1(y, Q^2) \tag{9}$$

$$\bar{g}_2(x, Q^2) \;\equiv\; g_2(x, Q^2) \;-\; g_2^{WW}(x, Q^2)\,. \tag{10}$$

For the QCD evolution of the structure function $g_1(x, Q^2)$ and twist-2 piece of $g_2(x, Q^2)$, the ordinary Dokshitzer-Gribov-Lipatov-Altarelli-Parisi (DGLAP) equation can be used. Here, we use the leading-order Fortran code provided by Saga group [29]. The flavor non-singlet and singlet channels are treated separately, since the mixing with the gluon distribution occurs in the latter. On the other hand, the Q^2-evolution of twist-3 distributions is known to be quite complicated due to mixing with quark-antiquark-gluon operators, the number of which increases rapidly with spin or the moment of the distributions. However, Ali, Braun and Hiller found that, in the large N_c limit, the Q^2-evolution of the chiral-even twist-3 flavor-nonsinglet distribution $\bar{g}_2(x, Q^2)$ is described by simple DGLAP type equation with slightly different forms for the anomalous dimensions from the twist-2 distributions [30]. Accordingly, the moments

of $\bar{g}_2(x,Q^2)$ obey the following simple equation :

$$\mathcal{M}_n[\bar{g}_2(Q^2)] \;=\; L^{\gamma_n^g/b_0}\,\mathcal{M}_n[\bar{g}_2(Q^2_{ini})]\,, \tag{11}$$

where $\mathcal{M}_n[g(Q^2)] \equiv \int_0^1 dx\, x^{n-1}\, g(x,Q^2)$, $L \equiv \alpha_S(Q^2)/\alpha_S(Q^2_{ini})$, $b_0 = \frac{11}{3}\,N_c - \frac{2}{3}\,N_f$, and

$$\gamma_n^g \;=\; 2\,N_c\,\left(\,S_{n-1} - \frac{1}{4} + \frac{1}{2\,n}\,\right)\,, \tag{12}$$

with $S_n = \sum_{j=1}^{n} \frac{1}{j}$. The Q^2-evolution of the corresponding distribution functions can be handled by the method described in [31]. In principle, the flavor-singlet part of $\bar{g}_2(x,Q^2)$ mixes with the gluon distribution, and the Q^2-evolution of it is not given by a simple equation as above even in the large N_c limit. In the following study, we shall neglect this mixing effect with gluons in the twist-3 flavor-singlet distributions, for simplicity. Finally, the total $g_2(x,Q^2)$ at the desired energy scale is obtained after combining the twist-2 and twist-3 pieces of $g_2(x,Q^2)$, which are evolved separately.

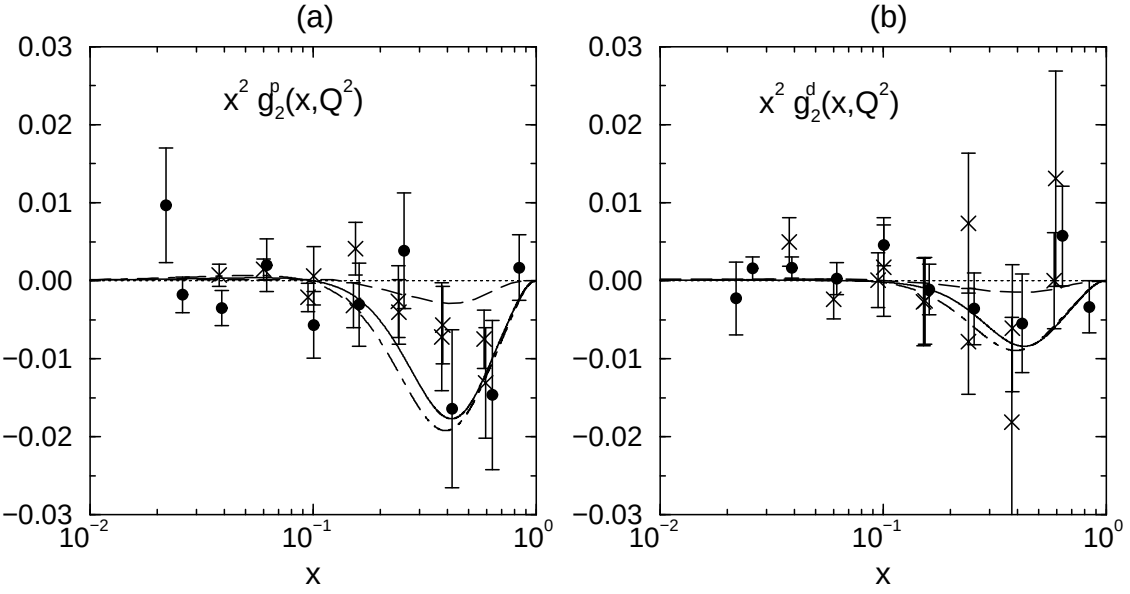

Figure 2: The theoretical structure functions $x^2\,g_2^p(x,Q^2)$ and $x^2\,g_2^d(x,Q^2)$ at $Q^2 = 5\,\mathrm{GeV}^2$ (solid curves) are compared with the corresponding E143 and E155 data (respectively shown by crosses and filled circles) as well as the predictions of Song's center-of-mass MIT bag model (dashed curves). The twist-2 parts of the theoretical structure functions (dash-dotted curves) are also shown for comparison.

We show in Fig.2 the theoretical structure functions $g_2(x,Q^2)$ at $Q^2 = 5\,\mathrm{GeV}^2$ for the proton (a) and the deuteron (b) in comparison with the corresponding experimental data. Here, the

crosses and the filled circles respectively stand for the E143 [32] and E155 data [33]. The final theoretical predictions for $g_2(x, Q^2)$ are represented by the solid curves, while their twist-2 part $g_2^{WW}(x, Q^2)$ are shown by the dash-dotted ones. The predictions of the center-of-mass MIT bag model by Song are also shown for the sake of comparison [18]. We point out that the predictions of the CQSM for both of $g_2^p(x, Q^2)$ and $g_2^d(x, Q^2)$ are relatively close to those of another version of MIT bag model given by Strattmann shown in [32] and sizably larger than those of Song's results. We also find that, according to the predictions of the CQSM, the differences between the full $g_2(x, Q^2)$ and their twist-2 parts are relatively small except for the smaller x region, although it is not clear from Fig.2 in which x^2 times $g_2(x, Q^2)$ are plotted. This tendency is also close to Stratmann's results rather than Song's results.

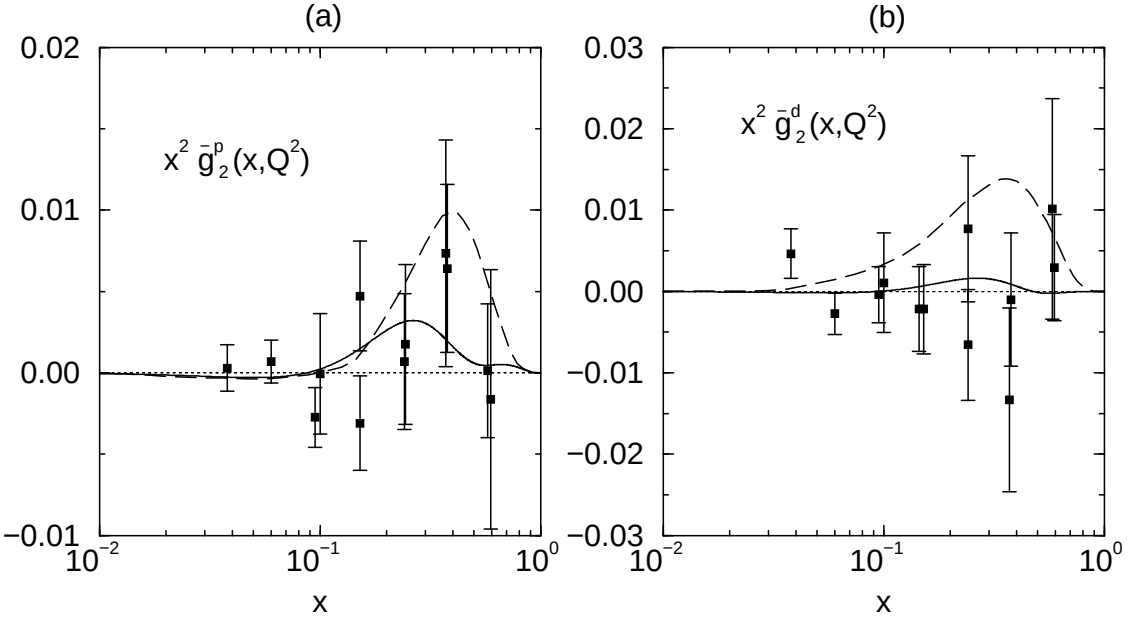

Figure 3: The twist-3 parts of the structure functions, $x^2\,\bar{g}_2^p(x, Q^2)$ and $x^2\,\bar{g}_2^d(x, Q^2)$ are compared with Song's predictions as well as the corresponding experimental data from his paper.

To see it more clearly, we show in Fig.3 our results for the twist-3 part of $g_2^p(x, Q^2)$ and $g_2^d(x, Q^2)$ in comparison with Song's predictions. Here, the solid curves are the predictions of the CQSM, while the dashed curves are those of the center-of-mass bag model by Song. The experimental data in this figure are from [18]. One clearly sees that the twist-3 parts of $g_2(x, Q^2)$ are much smaller in the CQSM than in Song's bag model calculation. Because of the large uncertainties of the available experimental data, it is difficult to say at the present moment which theoretical prediction is favored. Nonetheless, small twist-3 contributions to the spin structure functions $g_2(x, Q^2)$ appears to be favored by the recent E155 analysis of the

twist-3 matrix element :

$$d_2(Q^2) \;=\; 3\int_0^1 x^2\,\bar{g}_2(x,Q^2)\,dx \;=\; 2\int_0^1 x^2\,[\,g_1(x,Q^2) \;+\; \frac{3}{2}\,g_2(x,Q^2)\,]\,dx\,. \tag{13}$$

(Also interesting to notice here would be the fact that the instanton-liquid model of the QCD vacuum offers a qualitative explanation of the suppression of the twist-3 matrix element of $g_2(x,Q^2)$ relative to the twist-2 one [34].) We compare in Fig.4 the predictions of various theoretical calculations with the recent E155 data. As already shown in [33], the predictions of some models are apparently incompatible with the E155 analysis, although we must be cautious about difficulties in obtaining reliable and precise experimental information for these quantities. For instance, large and negative d_2 for the neutron predicted by the QCD sum rules [20, 21] apparently contradicts the E155 data. Similarly, large and negative d_2 for the proton predicted by the lattice QCD [22] seems incompatible with the E155 data.

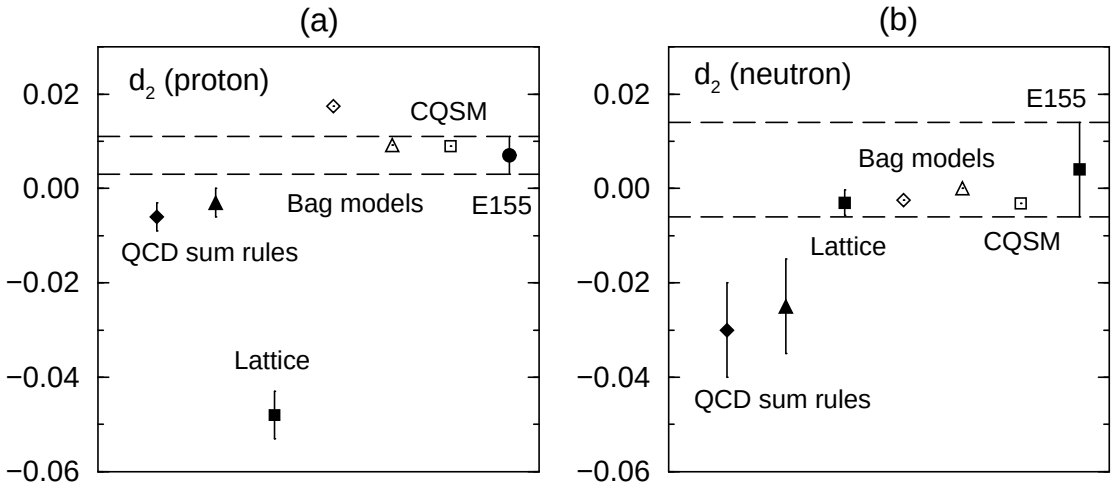

Figure 4: The predictions of various theoretical models for the twist-3 matrix element d_2 for the proton (a) and the neutron (b) are compared with the recent E155 analysis. Shown theoretical models are from left to right : QCD sum rules [20, 21], lattice QCD [22], MIT bag models [18, 16], and the CQSM.

On the other hand, the predictions of the CQSM as well as those of the MIT bag models seems consistent with the E155 data at least qualitatively. We see that the prediction of the naive MIT bag model for d_2^p is accidentally close to that of the CQSM. Its prediction $d_2^n = 0$ also seems to lie within the experimental error bars. Note however that the predictions of the naive MIT bag model must be taken with care, since the SU(6) structure of the bag wave function (this is the cause of the result $d_2^n = 0$ [16]) apparently contradicts large and negative behavior of the twist-2 neutron structure functions $g_1^n(x,Q^2)$ confirmed in several previous

experiments [10, 11, 12, 13]. This shortcoming of the original MIT bag model is remedied in Song's modified one, in which sizable SU(6) symmetry breaking effects are incorporated by hand, so that it reproduces both of $g_1^p(x, Q^2)$ and $g_1^n(x, Q^2)$ [18]. However, now we sees that the MIT bag model so refined gives a prediction for d_2^p, which is about two times larger than that of the CQSM and lies outside the errorbars of the E155 data. More precise experimental data are absolutely awaited for drawing more decisive conclusion about the twist-3 contributions to the nucleon spin structure functions, thereby selecting various models of nucleon internal structure.

To sum up, it has been shown in a series of paper [5, 6, 7] that the CQSM reproduces all the qualitatively noticeable features of the recent high-energy data for the twist-2 structure functions of the proton, the neutron and the deuteron, with *no adjustable parameter* except for the ititial energy scale of the DGLAP evolution equation. In the present investigation, we have extended this parameter-free analyses to the twist-3 spin structure function $g_2(x, Q^2)$. The theoretical predictions are shown to be consistent with the E143 and E155 measurements for $g_2^p(x, Q^2)$ and $g_2^d(x, Q^2)$ at $Q^2 = 5\,\mathrm{GeV}$, although the uncertainties of the existing experimental data are still too large to draw a decisive conclusion. We have also shown that the CQSM predicts very small twist-3 matrix elements d_2 for the proton and the neutron in conformity with the recent E155 analysis. The accumulation of more precise experimental data for $g_2(x, Q^2)$ as well as $g_1(x, Q^2)$ is absolutely necessary for more complete understanding of the nucleon spin structure.

Acknowledgement

The author would like to express his sincere thanks to Y. Koike for many helpful discussions concerning the scale dependence of the twist-3 distributions.

References

[1] EMC Collaboration, J. Aschman et al., Phys. Lett. B206 (1988) 364 ;
Nucl. Phys. B328 (1989) 1.

[2] NMC Collaboration, P. Amaudruz et al., Phys. Rev. Lett. 66 (1991) 2712.

[3] M. Wakamatsu and H. Yoshiki, Nucl. Phys. A525 (1991) 561.

[4] M. Wakamatsu, Phys. Rev. D46 (1992) 3762.

[5] M. Wakamatsu and T. Kubota, Phys. Rev. D60 (1999) 034020.

[6] M. Wakamatsu and T. Watabe, Phys. Rev. D62 (2000) 017506.

[7] M. Wakamatsu and T. Watabe, hep-ph/9912500, to appear in Phys. Rev. D.

[8] HERMES Collaboration, K. Ackerstaff et al., Phys. Rev. Lett. 21 (1998) 5519.

[9] E866 Collaboration, E.A. Hawker et al., Phys. Rev. Lett. 80 (1998) 3715.

[10] E143 Collaboration, K. Abe et al., Phys. Rev. D58 (1998) 112003.

[11] E154 Collaboration, K. Abe et al., Phys. Rev. Lett. 79 (1997) 26.

[12] E155 Collaboration, P.L. Anthony et al., hep-ex/994002.

[13] SMC Collaboration, B. Adeva et al., Phys. Rev. D58 (1998) 112001.

[14] R.L. Jaffe and X. Ji, Phys. Rev. D43 (1991) 724.

[15] M. Stratmann, Z. Phys. C60 (1993) 763.

[16] X. Ji and P. Unrau, Phys. Lett. B333 (1994) 228.

[17] F.M. Steffens, H. Hoffmann and A.W. Thomas, Phys. Lett. B358 (1995) 139.

[18] X. Song, Phys. Rev. D54 (1996) 1955.

[19] H. Weigel, L. Gamberg and H. Reinhardt, Phys Rev. D55 (1997) 6910.

[20] E. Stein, Phys. Lett. B343 (1995) 369.

[21] I. Balitsky, V. Braun and A. Klesnichenko, Phys. Lett. B242 (1990) 245 ;
B318 (1993) 648(E).

[22] M. Göckeler et al., Phys. Rev. D53 (1996) 2317.

[23] M. Wakamatsu and T. Watabe, Phys. Lett. B312 (1993) 184 ;
Chr.V. Christov, A. Blotz, K. Goeke, P. Pobylitsa, V.Yu. Petrov, M. Wakamatsu, and T. Watabe, Phys. Lett. B325 (1994) 467.

[24] M. Wakamatsu, Prog. Theor. Phys. 95 (1996) 143.

[25] P.V. Pobylitsa, M.V. Polyakov, K. Goeke, T. Watabe and C. Weiss, Phys. Rev. 59 (1999) 034024.

[26] B. Dressler, K. Goeke, P.V. Pobylitsa, M.V. Polyakov, T. Watabe, and C. Weiss, hep-ph/9809487.

[27] H. Burkhardt and W.N. Cottingham, Ann. Phys. (NY) 56 (1970) 453.

[28] S. Wandzura and F. Wilczek, Phys. Lett. 72B (1977) 195.

[29] M. Hirai, S. Kumano, and M. Miyama, Compt. Phys. Commun. 108 (1998) 38.

[30] A. Ali, V.M. Braun and G. Hiller, Phys. Lett. B266 (1991) 117.

[31] Y. Kanazawa and Y. Koike, Phys Lett. B403 (1997) 357.

[32] E143 Collaboration, K. Abe et al., Phys. Rev. Lett. 76 (1996) 587.

[33] E155 Collaboration, P.L. Anthony et al., Phys. Lett. B458 (1999) 529.

[34] J. Balla, M.V. Polyakov and C. Weiss, Nucl. Phys. B510 (1997) 327.